Powrie, W. & Batten, M. (2000). *Géotechnique* 50, No. 2, 127–140

# Comparison of measured and calculated temporary-prop loads at Canada Water Station

W. POWRIE* and M. BATTEN†

**The loads developed in tubular-steel temporary props during the construction of the London Underground Jubilee Line Extension (JLE) station at Canada Water were measured using vibrating-wire strain gauges. Prop temperatures were monitored and their influence on the prop loads assessed. Wall movements were also measured, by means of inclinometers. In this paper, the temperature-normalized prop loads are compared with the results of modified limit equilibrium calculations. Prop loads and wall movements are compared with the results of a series of parametric finite-element analyses carried out using the program CRISP. On the basis of the finite-element analysis results, the design assumptions giving the closest correlation between measured and calculated prop loads and wall movements are identified.**

**Les charges qui se développent dans les appuis temporai en acier tubulaire utilisés pendant la construction du proli gement de la ligne Jubilee dans le métro londonien (JLE la station Canada Water ont été mesurées en utilisant jauges de déformation à fil vibrant. Les températures appuis ont été étudiées et leur influence sur les charg imposées aux appuis a été évaluée. Les mouvements murs ont également été mesurés, au moyen de tubes inclir mètres. Dans cet exposé, nous comparons les charges sur appuis, à température normalisée, aux résultats des calc modifiés d'équilibre limite. Nous comparons les charg imposées aux appuis et les mouvements des murs a résultats d'une série d'analyses paramétriques d'élémer finis effectuées en utilisant le programme CRISP. Sur la ba des résultats des analyses d'éléments finis, nous identifio les hypothèses conceptuelles donnant la corrélation la pl étroite entre les charges mesurées et calculées et les mouv ments des murs.**

KEYWORDS: case history; field instrumentation; limit state design/analysis; monitoring; numerical modelling and analysis; retaining walls.

## INTRODUCTION

Field observations tend to suggest that there may often be a discrepancy between the loads actually developed in temporary props and those calculated using current methods of analysis (e.g. Glass & Powderham, 1994; Marchand, 1997). In this paper, some possible reasons for this apparent discrepancy are investigated with reference to temporary-prop loads measured during the construction of Canada Water Station on the London Underground Limited (LUL) Jubilee Line Extension (JLE).

Canada Water Station was built in a deep excavation, the sides of which were supported during construction by hard/soft secant-piled retaining walls. In the area of the research the excavation was approximately 17 m deep and the walls were supported at two levels by 1067 mm dia. tubular-steel props at 8·3 m centres. The loads in four of the props (two at each level) were monitored using a total of 32 vibrating-wire strain gauges (Geokon VK-4101), connected to a Campbell Scientific CR10 data logger. Four gauges, arranged at the quarter-points of the cross-section, were installed at both ends of each prop so that a full investigation of the strains in the prop, including those due to differential temperature effects, could be carried out. Thermistors were incorporated into the gauges, and readings of strain and temperature were taken at each gauge location at two-hourly intervals throughout the period (January–December 1995) the props were in place.

## GROUND CONDITIONS

### *Soil types*

There are six soil types present at Canada Water (Fig. 1): their main geotechnical parameters are summarized in Table 1. The Lambeth Group Sands and Clays and the Thanet Sands are significantly overconsolidated, while the Thames Gravel, alluvium and made ground are not. The geotechnical parameter have been derived primarily from the results of *in situ* and laboratory tests presented in the interpretative report associated with the JLE site investigation (Geotechnical Consulting Group 1991). The range of measured permeabilities ($k$) and soil stiffnesses ($E'$) was wide, as indicated in Table 1. The values given for the peak soil strength ($\varphi'_{peak}$) are either averages of those considered to be most representative. Soil strengths at the critical state ($\varphi'_{crit}$) have been estimated where possible from the relative density and the peak strength (Bolton, 1986) or from the plasticity index of the soil (Gibson, 1953). Where data from the site were not available, values were obtained from tests carried out on the same soil strata elsewhere in the Docklands area (Ferguson *et al.*, 1991; Howland, 1991; Ove Arup and Partners, 1991). The selection of soil parameters is discussed in more detail by Batten (1998).

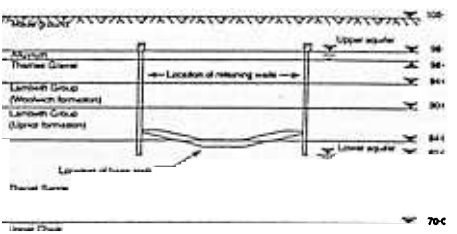

Fig. 1. Ground conditions showing approximate groundwater level during the construction of the station

### *Groundwater conditions*

There are two aquifers at the site; a shallow aquifer comprising the alluvium and the Thames Gravel, which lies above the (vertically) relatively impermeable Lambeth Group Clays, and a deep aquifer comprising the Lambeth Group Sands, the Thanet Sands and the Upper Chalk. During the construction period the piezometric level in the upper aquifer, within which

Manuscript received 30 June 1997; revised manuscript accepted 4 February 1999.
Discussion on this paper closes 4 August 2000; for further details see p. i.

* University of Southampton.
† TPS Consult, Croydon (formerly University of Southampton).

Table 1. Geotechnical parameters

| Soil type | Level at top of stratum: m TD* | $\rho$: kg/m$^3$ | $\varphi'_{peak}$: degrees | $\varphi'_{crit}$: degrees | $E'$: MN/m$^2$ | $k$: m/s | $K_0$ |
|---|---|---|---|---|---|---|---|
| Made ground | 105·5 | 1800 | 40 | 25 | 2–20 | $3{\cdot}6 \times 10^{-3}$ to $1{\cdot}6 \times 10^{-3}$ | 0·5 |
| Alluvium | 99·5 | 1850 | 28 | 25 | 2 | $1 \times 10^{-6}$ to $1 \times 10^{-5}$ | 0·8 |
| Thames Gravel | 98 | 2000 | 38 | 35 | 15–90 | $1 \times 10^{-4}$ to $1 \times 10^{-3}$ | 0·5 |
| Lambeth Group Clays | 94 | 2200 | 30 | 27 | 30–110 | $1{\cdot}2 \times 10^{-7}$ to $1{\cdot}3 \times 10^{-5}$ (h)‡<br>$1 \times 10^{-12}$ to $1 \times 10^{-11}$ (v) | 1·5 |
| Lambeth Group Sands | 90 | 2200 | 34 | 30 | 100–310 | $2{\cdot}8 \times 10^{-7}$ to $2{\cdot}8 \times 10^{-5}$ (h)<br>$1 \times 10^{-6}$ to $2{\cdot}8 \times 10^{-7}$ (v) | 1·5 |
| Thanet Sands | 84 | 2200 | 47 | 33 | 300–450† | $1{\cdot}9$ to $2{\cdot}3 \times 10^{-5}$ | 1·0 |

* All levels are expressed relative to the Tunnel Datum, TD, which is 100 m below Ordnance Datum (i.e. TD = OD + 100 m).
† The stiffness increases from a minimum at the top of the stratum to a maximum at the base of the stratum.
‡ (h) and (v) indicate permeabilities in the horizontal and vertical direction, respectively.

pore water pressures were hydrostatic, was approximately 98 m TD. The groundwater level in the lower aquifer was lowered to beneath the toe of the wall (82 m TD) during the construction of the station, to stabilize the base of the excavation. No data were available for the Lambeth Group Clays, but it is likely that the pore pressures within these relatively impermeable strata were in transition between the upper and lower aquifers.

## CONSTRUCTION DETAILS

Of the four props in which loads were monitored, two were at elevation 96 m TD (props U1 and U2) and two at elevation 89 m TD (prop L1, which was below prop U1, and prop L2, which was below prop U2). In the research area, the top of the wall was at 100 m TD. The 900 mm dia. reinforced concrete hard piles were installed at 1200 mm centres and were 18 m deep, giving a toe level of 82 m TD. The alternate 750 mm dia. soft piles were unreinforced and made from weaker concrete. They were installed to prevent the ingress of water from the upper aquifer and extended to 92 m TD—2 m below the top of the Lambeth Group Clays. The props were fabricated from 1067 mm dia. × 14·3 mm thick tubular-section, grade 65 steel and spanned 26·7 m between the secant pile retaining walls. Reinforced concrete waling beams cast against the wall reduced the free length of each prop to approximately 24·1 m (Fig. 2). The construction sequence is given in Fig. 3.

The 1 m thick reinforced concrete base slab, which was designed to act as a permanent prop, was poured beneath the props in the research area in early May 1995. The lower props were removed during June (prop L2) and July (prop L1) 1995 to allow the walls of the station box to be constructed. The upper props were removed in December 1995, after construction of an intermediate slab just below 96 m TD and backfilling of the void between the secant pile wall and the permanent structure.

## MEASURED PROP LOADS

There is sometimes a degree of confusion concerning the relationship between the reading of a vibrating-wire strain gauge and the load in the prop when the prop temperature changes, and whether any adjustment to the gauge reading is required. In general, the increase in prop load caused by an increase in temperature depends on the effectiveness of the prop end restraints, and is proportional (according to Hooke's law) to the *difference* between the strain in free expansion and the actual strain increment allowed by the movement of the support (Batten *et al.*, 1999).

Gauges having the same coefficient of thermal expansion as the prop respond directly to this strain difference, so that no adjustment to the measured strain (apart from multiplication by the Young's modulus $E$ and the cross-sectional area $A$) is required to obtain the prop load. Localized variations in strain will occur at each gauge owing to bending, temperature differences across the prop and/or fabrication irregularities, but the

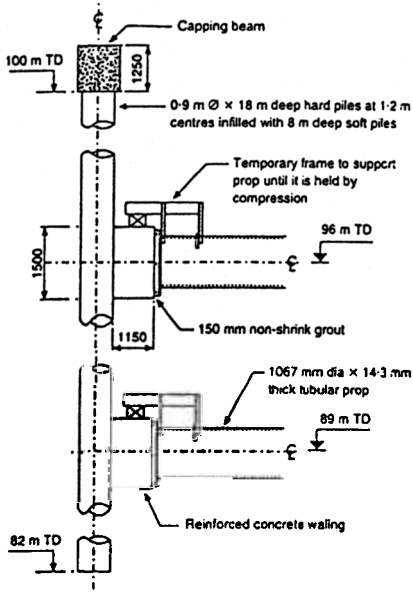


Fig. 2. Prop end details (excavation in cross-section) (dimensions in mm except where otherwise stated).

total axial load $P$ must be the same at each end of the prop and is most accurately calculated using the average of the strains indicated by the eight gauges, $\varepsilon_{av}$ (Batten *et al.*, 1999):

$$P = \varepsilon_{av} AE \qquad (1)$$

where $A = 0{\cdot}0473$ m$^2$ is the nominal cross-sectional area of steel in the prop and $E = 199 \times 10^6$ kN/m$^2$ is the (measured) Young's modulus of the steel.

### *Upper props*

Gauge datum readings should ideally be taken using a data logger when the prop is in an unloaded condition. Readings taken manually can be unreliable for establishing a strain datum (e.g. owing to the effects of nearby construction activities, vibrations or other disturbance) but should be acceptable for establishing a baseline temperature. Prop U1 was in a loaded condition when continuous monitoring began, and true datum readings had to be established when the prop was destressed prior to its removal (Fig. 4). Datum readings for prop U2 were taken before the prop was loaded and were checked following

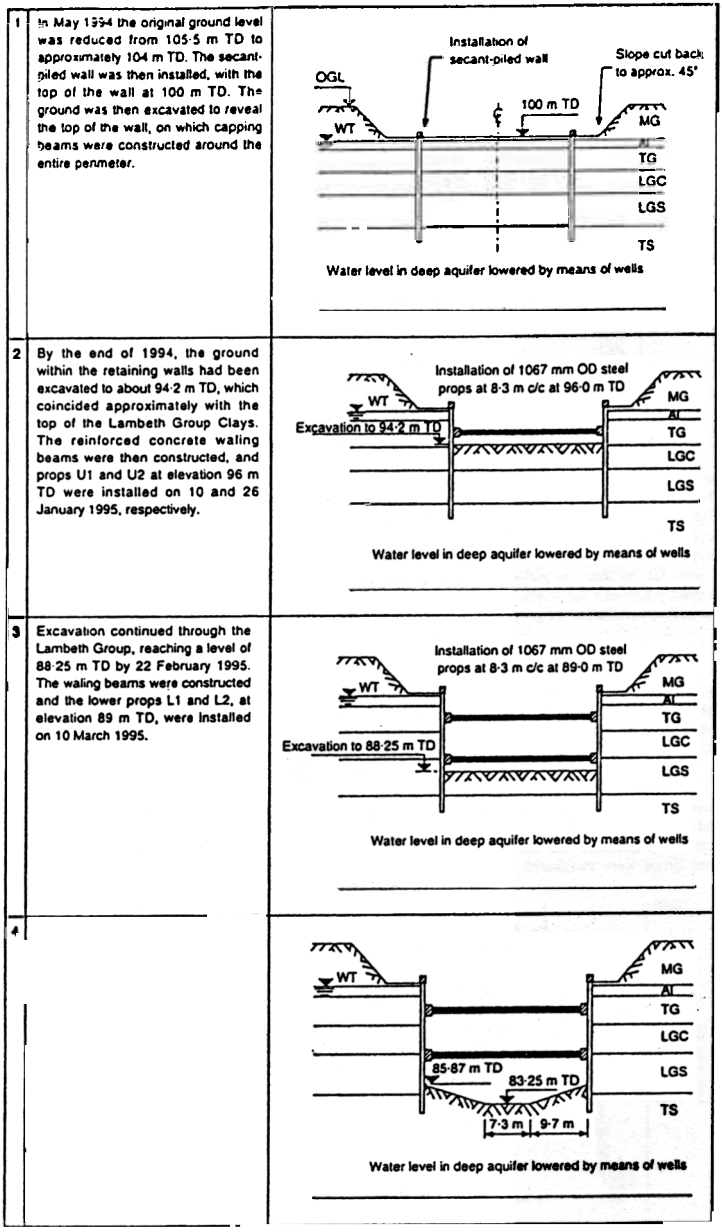


**Fig. 3. Summary of construction sequence (OGL, original ground level; WT, water table; MG, made ground; Al, alluvium; TG, Thames Gravel; LGC, Lambeth Group Clays; LGS, Lambeth Group Sands; TS, Thanet Sands)**

destressing prior to removal. Fig. 4 shows the axial load developed in each of the upper props as a function of time: zero time is 13 January 1995, the date on which prop load monitoring began. The absence of data over days 100–120 resulted from a problem with the computer used to download the data from the data logger.

The average loads measured in the upper props follow almost exactly the same trend, although the load in prop U1 was

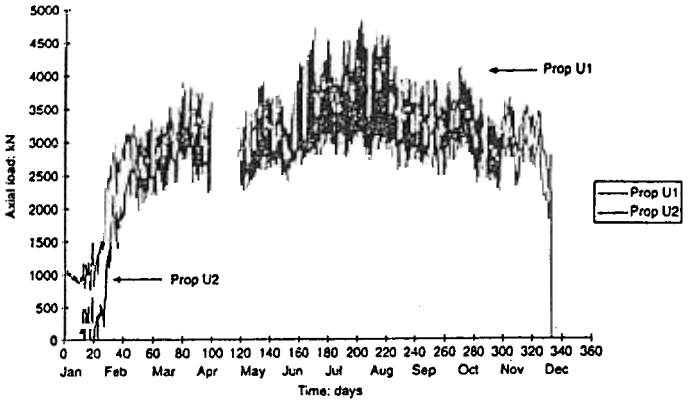


Fig. 4. Axial loads in upper props

consistently higher by approximately 400 kN. Prop U1 was installed 13 days before prop U2, and a compressive load of approximately 1000 kN had developed in prop U1 by the time prop U2 was placed. However, as the excavation progressed over the next 20 days, the load in prop U2 increased at a faster rate than that in prop U1 so that the difference in load was reduced. The discrepancy between the loads in the two props is probably due to the earlier installation of prop U1.

*Lower props*

Both lower props were installed on the same day and reliable datuma were established with the props in place but unloaded. The loads subsequently measured in the props were of a similar magnitude (Fig. 5).

*Effects of temperature on the prop loads*

Temperature and strain were recorded every two hours, enabling the effects of temperature on the prop loads to be investigated. The top props were monitored for almost a year, so that the full extent of seasonal temperature changes apparent. The variation in temperature indicated in Fig. 6 typical of the upper props.

The data presented in Figs 4 and 5 indicate the conside effect of temperature on the prop loads, with the load flu ing significantly with each daily cycle of temperature. fluctuations in load were greatest in the upper props durin summer months, when the difference between day and temperatures was largest. As would be expected, an increa temperature resulted in an increase in the compressive lo the prop, and a decrease in temperature resulted in a dec in compressive load.

During the summer when the excavation was at full d the variation in load in the top prop was typically 3 4575 kN (400–551 kN/m) for temperatures in the range 35°C. The lower props were removed before the summe the variations in load and temperature there were typ 1400–2300 kN (168–277 kN/m) and 6–19°C, respectively.

During the year in which the upper props were moni the temperature varied between approximately −4°C and (Fig. 6).* Taking the coefficient of thermal expansion fo

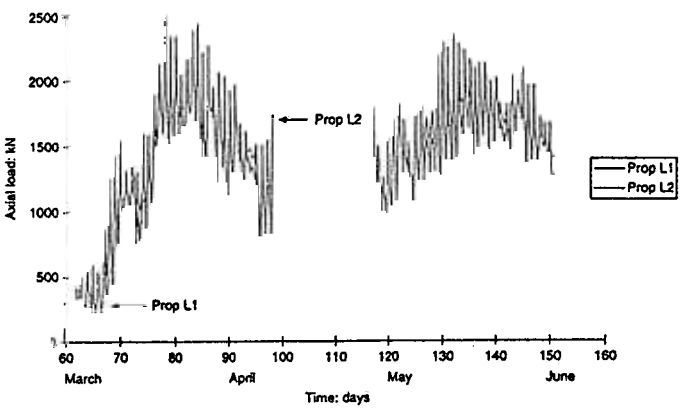


Fig. 5. Axial loads in lower props

* Temperatures were measured by a thermistor incorporated in the strain gauge housing, and may be a few degrees less than thos would have been measured by thermistors attached to the prop This is discussed by Batten *et al.* (1999).

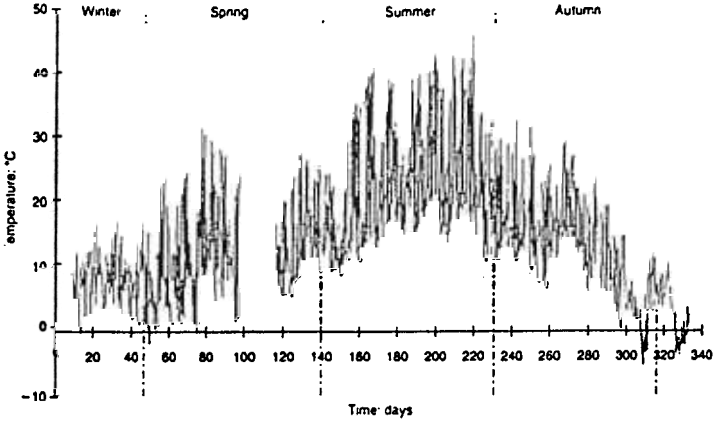


Fig. 6. Seasonal and daily variation in upper-prop temperature

prop steel as $11{\cdot}3 \times 10^{-6}$/°C, an increase in temperature of 50°C would, for an unrestrained prop 24·1 m long, result in an increase in length of 0·057% or 13·6 mm. Alternatively, if the prop were fully restrained, the increase in load would be 5318 kN.

Figure 7 shows values of measured strain $\varepsilon$ for an individual gauge reading (multiplied by $AE$ to give an apparent load in kN) plotted against the temperature, between days 192 and 280. During this time, no excavation or construction activity was carried out and variations in pore water pressures were minimal: an approximately linear relationship between temperature and measured strain is apparent. From Fig. 7, a temperature increase from approximately 7°C to 40°C caused the value of $EA\varepsilon$ to increase from approximately 2650 kN to 4700 kN. Had the prop been fully restrained an increase in temperature of 33°C would have resulted in an increase in $EA\varepsilon$ of 3476 kN. The data from this gauge therefore suggest partial restraint with an effectiveness of $2050/3476 \approx 59\%$.

The data from the other gauge locations also gave approximately linear relationships between temperature and measured strain, although the gradient of the line was different for each gauge. This is because the relationship between temperature and measured strain at each gauge location depends on the pattern of temperature change within the prop, the resulting response of the prop in biaxial bending, and possibly (for gauges on different props) the stiffness of the soil.

Biaxial bending due to differential temperature change is discussed by Batten *et al.*, 1996. The stiffness of the soil will depend on both the strain and the stress path followed, which will vary in turn with the excavation level and the relative movement of the wall. Also, there is some variation in ground conditions along the length of the excavation. Consequently, the relationship between measured strain and temperature is not strictly linear, and may well be different for each gauge. Taking all the gauges into account, the average effective restraint for the upper props was 52%: this is within the range for temporary props supporting stiff walls in stiff ground of 40–60% quoted by Twine & Roscoe (1997) on the basis of a number of case records. As the Lambeth Group Sands are stiffer than the Thames Gravels, and as a result of the geometry of the support system, the average effective restraint for the lower temporary props was rather greater at 63%.

Temperature-induced axial loads may account for a significant proportion of the total load carried by a prop installed at a low temperature. Although Twine & Roscoe (1997) showed that temperature-induced loads are unlikely to cause sudden failure

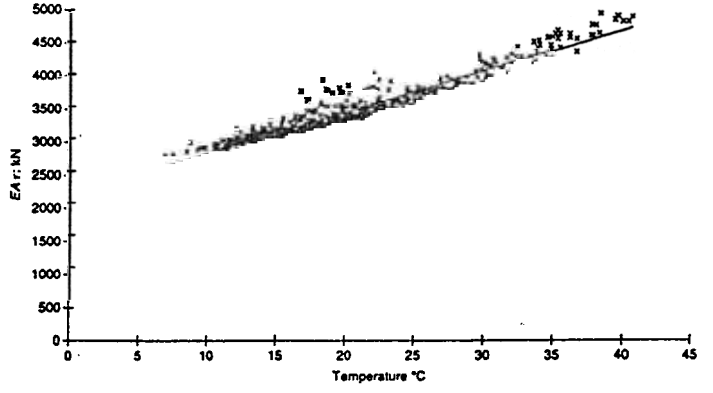


Fig. 7. Typical relationship between temperature and $AE\varepsilon$ for an individual gauge at a constant excavation level and with minimal pore water pressure variation

of ductile steel props, this does not apply to concrete props or brittle elements such as concrete end blocks, which must be designed for the full estimated temperature-induced load. Temperature-induced loads can be estimated from the anticipated temperature rise, the coefficient of thermal expansion of the prop and the degree of end restraint provided by the wall and the soil behind it. The data from Canada Water, together with other case histories reported by Twine & Roscoe (1997), suggest that for props near the crest of a stiff wall, the degree of end restraint could be of the order of 50%. A greater degree of restraint (~65% at Canada Water) should probably be expected for low-level props, but the range of temperature to which the prop is subjected may reduce with depth within the excavation.

*Reduction of temperature effects*

If the relationship between measured strain and temperature for each gauge with all other factors remaining constant is assumed to be approximately linear, the measured prop load (based on the average of the strain gauge readings—equation (1)) can be adjusted to account for temperature effects according to equation (2):

$$P_T = P_M - [(T_M - T_D) \times f] \quad (2)$$

where $P_T$ is the temperature adjusted load, $P_M$ is the measured load, $(T_M - T_D)$ is the average temperature rise above the gauge datum temperatures (i.e. the gauge temperatures when the prop started to take up load) and $f(= dP/dT)$ is an adjustment factor determined from the average load/temperature relationship. Compressive loads are taken as positive.

Equation (2) gives an estimate of the loads that would have been recorded in each prop had the excavation been made without variation in temperature. These are shown in Fig. 8. As temperature effects are not usually considered explicitly in retaining-wall analyses, the temperature-adjusted loads shown in Fig. 8 form a suitable basis for a comparison between measured and calculated prop loads.

Although the fluctuations in prop load due to temperature are considerably reduced in Fig. 8, they have not been entirely eliminated. This is due to the prop load/temperature relationships not being truly linear, and to the seasonal variations in differential temperature across the prop. Nevertheless, the remaining changes in prop load can largely be related to construction events and changes in pore water pressure (Batten, 1998).

## LIMIT EQUILIBRIUM ANALYSIS

*Procedure*

Limit equilibrium analyses were carried out, assuming the development of active conditions in the soil behind the wall and passive conditions in the soil in front. This was considered reasonable, owing to the relatively small embedment depth and the fact that most of the excavation took place with either no or only one level of temporary props in place. As a result of the stress paths followed by the soil during the installation of an *in situ* concrete wall, it is likely that only a small amount of wall movement will be required for the retained soil to reach the active state—even if the initial lateral earth pressure coefficient is high (Powrie *et al.*, 1998). The shallow depth of embedment means that the shear strain in the soil in front of the wall is large in comparison with the rotation of the wall (Bolton & Powrie, 1988): this, together with the effects of overburden removal during excavation, is likely to result in the relatively rapid mobilization of passive or near-passive earth pressures in the soil in front of the wall.

The actual excavated profile at formation level cannot easily be modelled in a simple limit equilibrium analysis, because of the battered sides: the base of the excavation was therefore taken to be horizontal at a level of 84·4 m, which was considered to represent an appropriate average.

The soils at Canada Water were generally granular with relatively high permeabilities and therefore the wall behaviour was analysed in terms of the fully drained effective stresses. This type of analysis may, however, underestimate the short-term shear strength of the lower-permeability Lambeth Group Clays (see Table 1), if in reality they remain substantially undrained during the time the props are in place.

In the retained soil hydrostatic conditions were assumed in the Thames Gravels below a measured piezometric level of 98·5 m TD. Pore water pressures were assumed to return to zero through the relatively impermeable Lambeth Group Clays (Fig. 9). The groundwater level in the lower aquifer was drawn down to below the toe of the wall, and pore water pressures in the Lambeth Group Sands and Thanet Sands were therefore set to zero in the analyses.

Two construction stages were considered: (*a*) with the excavation at formation level and both the upper and lower temporary props in place, and (*b*) after the permanent concrete prop had been poured and the lower prop removed (Fig. 9).

The earth pressure coefficients $K_a$ and $K_p$ were taken from Caquot & Kerisel (1948), assuming that the soil/wall friction angle $\delta$ was equal to $\varphi'_{crit}$ on both sides of the wall. This was

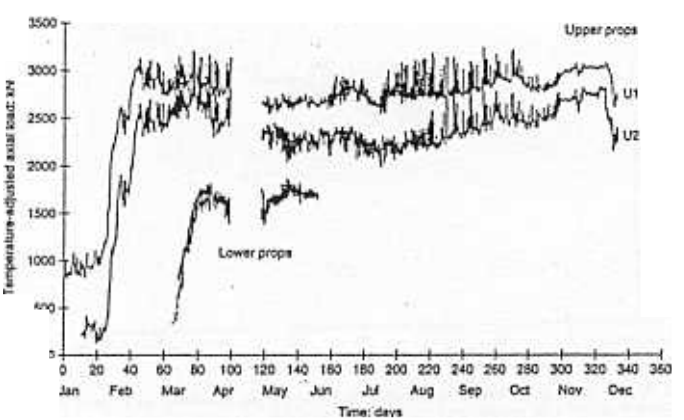


**Fig. 8. Temperature-adjusted prop loads**

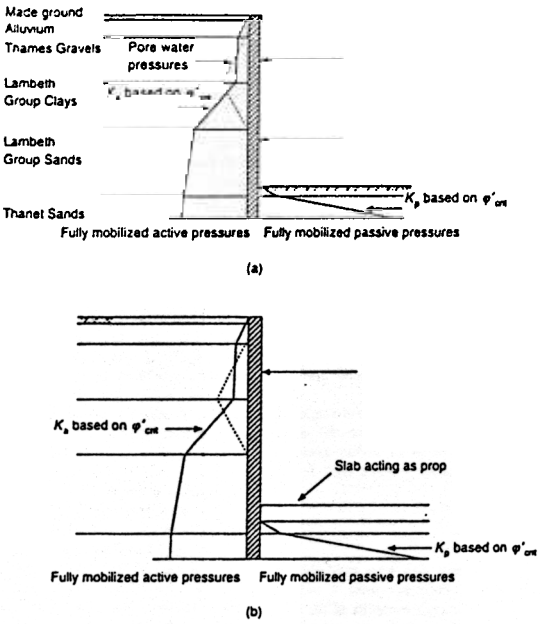


**Fig. 9. Stages of limit equilibrium analysis showing idealized effective-stress distribution: (a) excavation to formation level; (b) permanent prop slab cast and lower temporary prop removed**

considered to be reasonable on the basis of the roughness of the secant-piled wall and the probable directions of relative soil/wall movement in this case. Also, these assumptions seem to provide a reasonable indication of the onset of large deformations for embedded retaining walls that are either unpropped or propped at a single level near the crest (Powrie, 1996).

*Results*

The calculated loads are compared with the measured prop loads (adjusted for temperature effects) in Table 2. Despite the approximate nature of the analysis, prop loads close to those actually developed were calculated for the two construction stages considered. The calculated prop loads are, however, extremely sensitive to the excavation depth, with a change in formation level of just 0·1 m causing variations of approximately 9% and 30% in the upper and lower prop loads, respectively. Had the formation level been taken as (say) 84·5 m, therefore, the calculated prop loads would not have been as close to the measured values. Also, if the depth of embedment of the wall had been greater, the assumption of fully mobilized passive pressure in the soil in front of the wall would probably not have been reasonable. The limit equilibrium analyses are discussed later in the paper, in comparison with the results of the finite-element analyses.

## FINITE-ELEMENT ANALYSES

A series of finite-element analyses was carried out, assuming plane strain conditions, using the program CRISP (Britto & Gunn, 1987). Each of the six soil types was modelled as an elastic/Mohr–Coulomb plastic material with fully coupled consolidation.

*Finite-element mesh and boundary conditions*

Since the idealized geometry of a cross-section through the excavation is symmetrical about the centre line, the finite-element mesh represented one half of the excavation (Fig. 10). The lower horizontal boundary of the mesh was set at the interface between the Thanet Sands and the underlying chalk, which was assumed to be incompressible. The far vertical boundary was set at 60 m from the wall, which was considered to be sufficiently remote for changes in stress and strain to

**Table 2. Comparison of actual and calculated prop loads—limit equilibrium analysis**

| | | Upper prop | | Lower prop | |
|---|---|---|---|---|---|
| | | kN | kN/m | kN | kN/m |
| Excavation to formation level | Calculated | 2720 | 328 | 1740 | 210 |
| | Measured | 2658 | 320 | 1639 | 203 |
| Permanent prop cast and lower temporary prop removed | Calculated | 3223 | 388 | – | – |
| | Measured | 2900 | 349 | – | – |

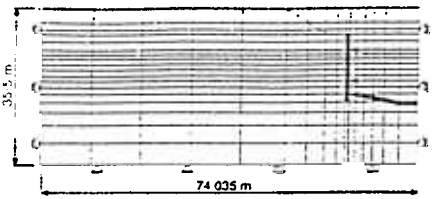


Fig. 10. Finite-element mesh

be negligible.* The vertical boundaries were fixed in the horizontal direction, but were free to move vertically. The lower horizontal boundary was fixed in both the vertical and the horizontal direction.

The soil, the wall and the concrete base slab were modelled using eight-noded quadrilateral elements, except for the occasional use of six-noded triangular elements to define some of the excavated profiles. Consolidation elements were used for all of the soil strata.

*Structural components*

The reinforced concrete wall and base slab were modelled as impermeable elastic materials with a Poisson's ratio $\nu' = 0{\cdot}15$ and a unit weight of 24 kN/m$^3$. The Young's modulus of the slab was specified as $22{\cdot}9 \times 10^{-6}$ kN/m$^2$ to give the same bending stiffness ($EI$) per metre run as the actual composite structure. The Young's modulus of the wall was taken as $22 \times 10^6$ kN/m$^2$, representing the reinforced (hard) piles only. The intermediate (soft) piles were ignored since their strength and stiffness were comparatively insignificant. In the analyses a uniform wall thickness of 0·685 m was used, which gives the same bending stiffness per metre run as the 0·9 m dia. hard piles at 1·2 m centres used in reality. The connection between the wall and the slab was modelled as a pinned joint unable to transmit bending moments. In reality this was a butted joint which would be capable of transmitting bending moments, provided that the interface between the wall and the slab remained in compression. Although the assumption of a pinned joint may lead to an overprediction of long-term wall bending moments and deflections, there is unlikely to be any significant effect on the calculated short-term loads in either the temporary or the permanent props (Powrie & Li, 1991).

The temporary props were modelled in the analyses using 2 m long bar elements with a reduced Young's modulus, giving a stiffness in axial compression (per metre run) equivalent to 1067 mm dia. × 14·5 mm thick steel props at 8·3 m centres, spanning 13·35 m (the half-width of the excavation).

*Wall installation effects*

The effects of wall installation at Canada Water were investigated by means of an axisymmetric finite-element analysis simulating the installation of a single pile, as described in the Appendix.

Although an axisymmetric analysis may underestimate the stress changes due to the installation of a complete wall, it has been shown to give results closer to the actual stress changes measured in the field than those of a plane strain analysis, which tends to overestimate wall installation effects (Higgins *et al.*, 1989). The reduction in the piezometric level in the lower aquifer from the *in situ* value to 82 m TD was also modelled in the axisymmetric analysis of the installation of a single pile. The earth pressure coefficients at the end of the axisymmetric analysis were specified as the pre-excavation values at the start of the plane strain analysis of the main excavation sequence. Removal of the pile casing was likely to have caused a loosening of the Thames Gravels: wall installation effects in this stratum were therefore modelled by using the lower-bound value of $20 \times 10^3$ kN/m$^2$ for the Young's modulus.

The main shortcoming of the method used to model wall installation effects was that the post-installation earth pressure coefficients had to be applied across the entire mesh. It is considered, however, that the error this causes is small, because the behaviour of the wall is influenced primarily by the soil closest to it. A possible alternative approach to modelling the effects of installing a diaphragm wall panel suggested by Ng *et al.* (1995) was not adopted, because its applicability to bored pile walls is uncertain. Furthermore, the Ng *et al.* (1995) method results in an increase in lateral stress below the toe of the wall, which may not be apparent when the installation of a series of adjacent panels to form a complete wall is modelled (Gourvenec, 1998).

*Groundwater levels*

The analyses were carried out assuming that a line of zero gauge pore water pressure in the retained soil was maintained at a level of 98 m TD. The initial pore water pressures specified were those at the end of the axisymmetric analysis, which included the effect of lowering the groundwater level in the deep aquifer. The pore water pressure at the excavated soil surface was set to zero at each stage of the excavation. Pore water pressures elsewhere within the mesh were calculated by the program on the basis of the elapsed time following a change in boundary stress or pore water pressure and the consolidation characteristics of the soil.

*Soil parameters*

A total of five analyses was carried out to investigate the sensitivity of the temporary-prop loads to various soil parameters and input assumptions. The conditions and soil parameters used in each analysis are summarized in Table 3. (The made ground was removed prior to excavation between the retaining walls. The soil parameters for this stratum were the same in all of the finite-element analyses, and were as given in Table 1 with $\varphi' = 25°$, $E' = 10$ MPa and $k = 8 \times 10^{-4}$ m/s).

The elastic Young's moduli used to describe the stress–strain behaviour of the soils prior to failure were not strain-dependent; hence the effects of a reduction in soil stiffness with increasing strain could not be modelled. Experience has shown, however, that satisfactory wall movements and structural stress resultants (but not soil settlements) can be calculated for retaining walls in stiff overconsolidated clays using a simple elastic/Mohr–Coulomb plastic soil model, provided that the elastic modulus is chosen with care (Burland & Kalra, 1986; Powrie *et al.*, 1999). The values of Young's modulus shown in Table 3 were derived from the site investigation data as detailed by Batten (1998) and are considered to be relevant to the strains typically associated with embedded retaining walls in practice.

*Prop loads*

The maximum temporary-prop loads calculated in the five analyses are given in Table 4. The results indicate that the prop loads, particularly those in the upper props, are most sensitive to the pre-excavation stress condition (case 5) and the permeability of the Lambeth Group Clays (case 4). In the analysis in which wall installation effects were not taken into account (case 5), prop loads significantly in excess of those measured were calculated. In the upper props the calculated loads were 64% greater than those measured, while in the lower props the discrepancy was 54%.

The permeability of the Lambeth Group Clays influences the

* Page (1995) carried out two-dimensional finite-element analyses of diaphragm wall trench excavations 18 m deep with first stress- and then strain-controlled boundaries at a distance of 52·5 m from the excavation, with no significant difference in the results.

Table 3. Soil parameters and other assumptions used in finite-element analyses

| Case | Description of conditions | Soil | $\phi'$ | $E'$: MN/m$^2$ | $k$: m/s |
|---|---|---|---|---|---|
| Case 1 (standard) | Upper-bound (peak) values for shear strength<br>Upper-bound values for Young's modulus<br>Minimum permeability of Lambeth Group Clays in both vertical and horizontal directions<br>Wall installation effects | Al | 28° | 2 | |
| | | TG | 38° | 20 | |
| | | LGC | 30° | 150 | |
| | | LGS | 34° | 310 | |
| | | TS | 47° | 300–450* | |
| Case 2 | *Lower-bound (critical-state) values for shear strength*<br>Upper-bound values for Young's modulus<br>Minimum permeability of Lambeth Group Clays in both vertical and horizontal directions<br>Wall installation effects | Al | 25° | 2 | |
| | | TG | 35° | 20 | |
| | | LGC | 27° | 150 | |
| | | LGS | 30° | 310 | |
| | | TS | 33° | 300–450 | |
| Case 3 | Upper-bound (peak) values for shear strength<br>*Average values for Young's modulus*<br>Minimum permeability of Lambeth Group Clays in both vertical and horizontal directions<br>Wall installation effects | Al | 28° | 2 | |
| | | TG | 38° | 20 | |
| | | LG | 30° | 70 | |
| | | LG | 34° | 200 | |
| | | TS | 47° | 300–450 | |
| Case 4 | Upper-bound (peak) values for shear strength<br>*Upper bound values for Young's modulus*<br>*Maximum permeability of Lambeth Group Clays in both vertical and horizontal directions*<br>Wall installation effects | Al | 28° | 2 | |
| | | TG | 38° | 20 | |
| | | LGC | 30° | 150 | |
| | | LGS | 34° | 310 | |
| | | TS | 47° | 300–450 | |
| Case 5 | Upper-bound (peak) values for shear strength<br>Upper-bound values for Young's modulus<br>Minimum permeability of Lambeth Group Clays in both vertical and horizontal directions<br>*Wall installation effects ignored* | Al | 28° | 2 | |
| | | TG | 38° | 90 | |
| | | LGC | 30° | 150 | |
| | | LGS | 34° | 310 | |
| | | TS | 47° | 300–450 | |

* The stiffness for the Thanet Sands increases from a minimum at the top of a stratum to a maximum at the base of the stratum.
† (h) and (v) indicate permeabilities in the horizontal and vertical direction, respectively.

Table 4. Maximum calculated prop loads

| Case | Load in upper prop | | Load in lower prop | |
|---|---|---|---|---|
| | kN | kN/m | kN | kN/m |
| 1 | 3450 | 416 | 1890 | 228 |
| 2 | 3670 | 442 | 3000 | 361 |
| 3 | 3910 | 471 | 2180 | 263 |
| 4 | 4465 | 538 | 2190 | 264 |
| 5 | 4930 | 594 | 2690 | 324 |
| Maximum measured loads (approx., with temperature effects removed) | 3000 | 361 | 1750 | 211 |
| Limit equilibrium analysis | 3220 | 388 | 1740 | 210 |

degree of consolidation that takes place during construction and, consequently, the shear resistance of the soil. When the permeability of the Lambeth Group Clays was increased so that this stratum behaved in a substantially drained manner (i.e. the negative excess pore water pressures induced on excavation dissipated fully during the construction period—case 4), the loads calculated in the upper and lower props were greater than those measured by approximately 50% and 25%, respectively.

Prop loads closest to the measured values were calculated by taking the effects of wall installation into account and using the minimum permeability of the Lambeth Group Clays in both the horizontal and the vertical direction (case 1).

The results of case 3 indicate that soil stiffness also has an effect on the prop loads. Although only the stiffnesses of the Lambeth Group Sands and Clays were reduced, prop loads up to about 15% greater than in the case 1 analysis were calculated. The increase in the calculated wall movement following installation of the upper props was about 33%.

Initial comparison of the results from cases 1 and 2 suggests that the prop loads, particularly in the lower props, were overestimated when critical-state (as opposed to peak) strengths were used. However, this is mainly due to the large difference between the critical-state and peak strengths of the Thanet Sands. One further analysis was carried out using peak strengths in all strata except the Thanet Sands, in which the critical-state strength was specified: the calculated upper and lower prop loads were 3602 kN and 2979 kN, respectively, which are similar to the loads calculated for case 2, where critical-state shear strengths were used in all strata.

If the mobilized shear strength in the Thanet Sands in the

case 1 analysis is examined (Fig. 11), it is apparent that it exceeds the critical-state value only in front of the wall, where the maximum frictional strength mobilized is 42°. Behind the wall the maximum frictional strength mobilized is 30°, which is less than the critical-state value of 33°. (Fig. 11 relates to the mid-depth of the Thanet Sands at a distance of 0·11 m behind and in front of the wall).

Figure 12 shows that the prop loads calculated in the case 1 analysis were generally within approximately 15% of the temperature-adjusted measured loads. The analysis, however, did not calculate the reduction in the upper-prop load between day 91 (when the final excavation level was reached) and day 188 (when the lower prop was removed). This is probably because increases in load in the concrete base slab (which was poured on day 118), due to thermal expansion during cement hydration, were not modelled. The temporary-prop loads measured at Canary Wharf (Batten, 1998) suggest that with a thick base slab the effect of this can be quite significant.

The gradual increase in the upper-prop calculated load between day 91 (when the full excavation depth was reached) and day 333 (when the upper prop was removed) can be explained with reference to the pore water pressures in the low-permeability Lambeth Group Clays behind the wall (Fig. 13). These gradually became more negative as the excavation progress until day 76, when the excavation neared completion. After t time the gradual dissipation of the negative excess pore wa pressures resulted in a corresponding increase in the prop loa The pore water pressures had still not reached their equilibri values at the end of the analysis.

There is reasonable agreement between the prop loads calc lated in the case 1 finite-element analysis and using the lin equilibrium approach. However, this must have been fortuito at least to some extent, because there are significant differenc in detail between the two analyses. In the limit equilibriu analysis, long-term equilibrium pore water pressures were a sumed (Fig. 9(a)), whereas in the finite-element analysis t pore water pressures in the Lambeth Group Clays were substa tially negative (Fig. 13). Also, critical-state soil strengths we assumed in all strata in the limit equilibrium analyses, while the case 1 finite-element analysis a strength in excess of t critical-state value was mobilized in the Thanet Sands in fro of the wall.

Both of these differences would tend to reduce prop load whereas the prop loads calculated in the case 1 finite-eleme analysis were 7–9% greater than those given by the lim equilibrium method. This discrepancy is explained by the fa

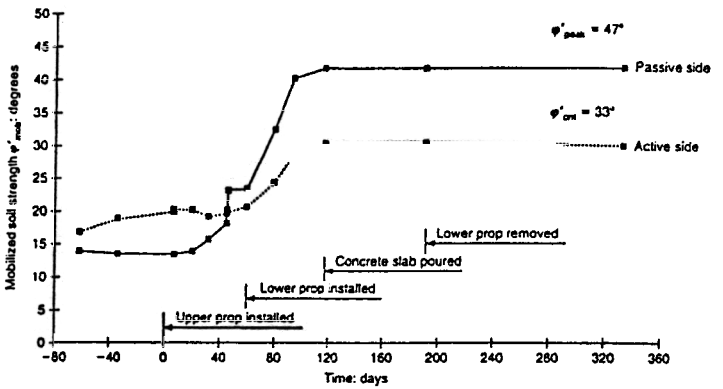


Fig. 11. Soil strength mobilized in Thanet Sands—case 1 finite-element analysis

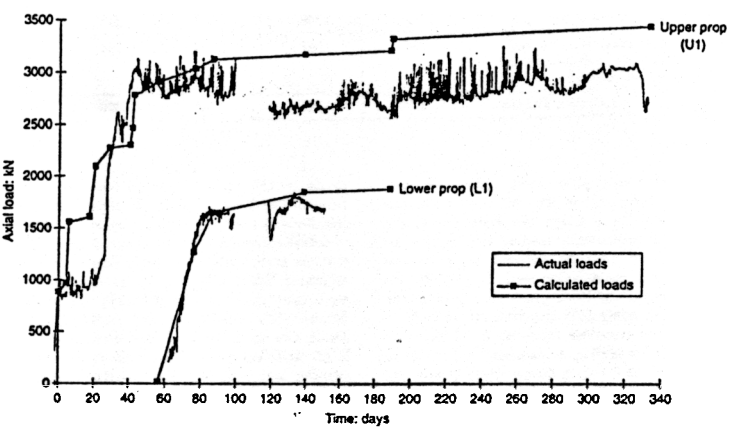


Fig. 12. Comparison of actual and calculated prop loads—finite-element analysis, case 1

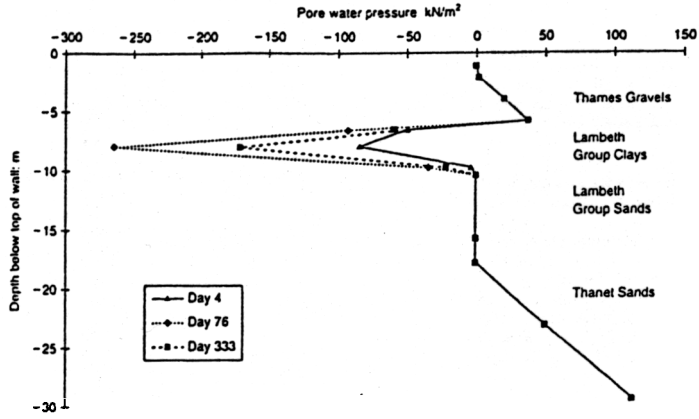


Fig. 13. Pore water pressures behind wall, case 1 finite-element analysis

that in the finite-element analysis the soils behind the wall (except for the Lambeth Group Sands) were generally not at failure, resulting in higher than active lateral effective stresses and an overall increase in prop loads compared with the limit equilibrium calculation.

A comprehensive understanding of the factors actually governing the loads in the temporary props in the field is not really possible without measuring the effects on the soil of wall installation and the transient pore water pressures in low-permeability strata. Unfortunately, financial and time constraints precluded the installation of the instrumentation that this would have required at Canada Water. It is therefore uncertain whether the assumptions made in the case 1 finite-element analysis (relatively slow dissipation of negative pore water pressures and soil stiffnesses insufficient to mobilize fully active pressures behind the wall) are more or less realistic than those made in the limit equilibrium calculation (long-term pore water pressures and fully active conditions behind the wall). Clearly there is a need for future monitoring exercises to consider the behaviour of the soil as well as the retaining system, despite the additional costs and difficulties this will entail.

*Wall movements*

The wall movements calculated in the case 1 analysis, following installation of the upper prop, are compared in Fig. 14 with the wall movements measured using an inclinometer tube installed in the wall. The wall movements measured above the level of the upper props are unreliable, owing to a lack of fixity of the inclinometer tube through the capping beam. Apart from this, the agreement is generally close, although the actual wall movements include temperature effects whereas the calculated wall movements do not.

Comparison of the calculated wall movements shown in Fig. 14 with those from the other finite-element analyses (Batten, 1998) shows the soil stiffness to be the main factor affecting wall displacements, which were increased by approximately 33% when the stiffnesses of the Lambeth Group Strata were reduced (case 3). This is qualitatively consistent with the results of previous finite-element analyses, e.g. Powrie & Li (1991). The soil strength parameters did not have a significant influence on the calculated wall movements.

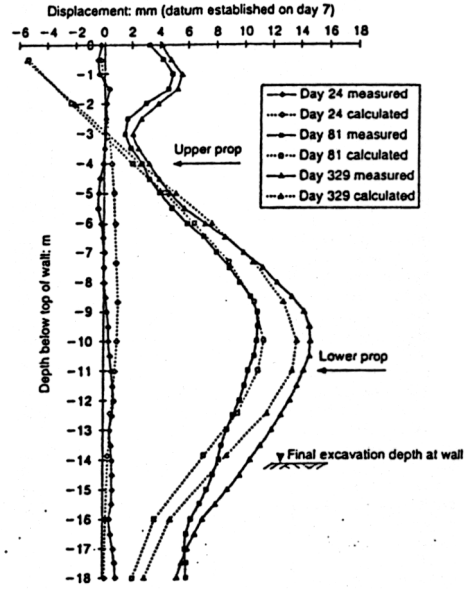


Fig. 14. Comparison of measured and calculated wall movements

## CONCLUSIONS

The temporary-prop loads and wall movements measured during the construction of the Jubilee Line Extension station at Canada Water have been compared with those calculated in a series of finite-element analyses carried out to investigate the effects of wall installation and uncertainties in the soil strength, stiffness and permeability. Temporary-prop loads and wall movements closest to those measured were calculated in finite-element analyses in which

(*a*) the changes in lateral stress due to secant pile wall installation were taken into account
(*b*) soil stiffnesses at the upper end of the measured or estimated range were specified
(*c*) the soil strength mobilized in the soil remaining in front of the wall (the Thanet Sands) was allowed to exceed the

estimated critical-state value (but not the estimated peak value)

(*d*) the permeability of the Woolwich and Reading Clays was reduced so that dissipation of negative excess pore water pressure was only about 35% complete at the end of the modelled construction sequence.

The calculated prop loads were then about 15% greater than the measured loads, discounting increases in load due to increases in temperature.

Limit equilibrium calculations, in which fully active conditions were assumed behind the wall and fully passive conditions in front, were carried out at two stages: (*a*) just before placement of the permanent prop slab, and (*b*) just after removal of the lower temporary props. The results of these calculations were in close agreement with the measured prop loads. However, this must have been fortuitous to some extent because

(*a*) in contrast to the implication of the results of the finite-element analyses, fully drained conditions had been assumed in the Woolwich and Reading Clays

(*b*) the prop loads calculated by the limit equilibrium analysis were very sensitive to the equivalent excavated depth used.

Also, the assumption of fully passive conditions in the soil remaining in front of the wall would probably not have been justified for a wall with a substantially deeper embedment.

Temperature-induced axial loads may account for a significant proportion of the total load carried by a prop installed at a low temperature and must be considered in design, particularly if elements of the propping system are brittle (e.g. concrete end blocks). Temperature-induced loads can be estimated from the anticipated temperature rise, the coefficient of thermal expansion of the prop and the degree of end restraint provided by the wall and the soil behind it. For props near the crest of a stiff wall, the degree of end restraint could be of the order of 50%. Low-level props might be restrained with an effectiveness of perhaps 65%, but the range of temperature experienced by a prop may reduce with depth within the excavation.

For stiff reinforced concrete retaining walls of the type used at Canada Water, it therefore seems that temporary-prop loads similar to those measured in the field (neglecting temperature effects) can be calculated using limit equilibrium and finite-element analysis, provided that appropriate soil parameters and input assumptions are used. Although in design a margin of safety is essential to allow for events such as the accidental removal of a prop, the apparent overprediction of prop loads is probably the result of a consistently conservative set of design assumptions rather than any flaw in the underlying soil mechanics principles.

To clarify the real impact of uncertainties such as wall installation effects and transient pore water pressures in low-permeability strata, there is a need for further field studies in which the behaviour of the soil is monitored as closely as that of the support system.

ACKNOWLEDGEMENTS

The work described in this paper was carried out with the support of the Engineering and Physical Sciences Research Council (EPSRC), Bachy, CIRIA, Kvaerner, Ove Arup and Partners, Tarmac Construction and Wimpey Construction. The authors are grateful to David Beadman, Roger Boorman, Ted Chaplin, Fin Jardine, Quentin Leiper, Richard McGivern, Derek Robertson, Michael Sansom, David Twine and Hai-Tien Yu for their advice and encouragement during the course of the research, and to London Underground Limited for permission to publish this paper.

## APPENDIX. AXISYMMETRIC ANALYSIS OF THE INSTALLATI OF A SINGLE PILE

### *Finite-element mesh and parameters*

The finite-element mesh used in the axisymmetric analysis of t installation of a single pile consisted of eight-noded quadrilate elements which became gradually smaller towards the pile, where t changes in stress and strain were more significant. The lower horizon boundary of the mesh was set at the interface between the Thanet Sa and the underlying chalk and was fixed in both the horizontal and t vertical directions. The far vertical boundary was 60 m from the out surface of the pile. Both vertical boundaries were fixed in the horizon direction, allowing vertical movement only. The upper surface of t mesh was at 100 m TD, the 5·5 mm of made ground above this bei modelled as a surcharge of 97 kPa (Fig. 15).

The concrete of the single 0·9 m dia. hard pile was modelled as . impermeable linear elastic material with a Young's modulus ($E$) · $22 \times 10^6$ kPa and a unit weight ($\gamma$) of 24 kN/m$^3$.

All soils were modelled as consolidating elastic/Mohr–Coulon plastic materials. The values of the soil parameters used in th axisymmetric analysis are given in Table 5.

Throughout the analysis a line of zero pore water pressure w. maintained at the top of the Thames Gravels at 98 m TD, th approximate *in situ* piezometric level of the upper aquifer. Hydrostat conditions were assumed to apply through the Thames Gravels to the t of the Lambeth Group Clays at 94 m TD. At the *in situ* stage the po water pressures in the lower aquifer were taken to be hydrostatic belo 90 m TD, at which level the initial pore water pressure was set to 39 kl (Fig. 16), consistent with a groundwater level in the lower aquifer 94 m TD. Thus the initial pore water pressure was set at 39 kP throughout the Lambeth Group Clays.

### *Modelling wall installation*

The first stage of construction was the installation of the temporar support casing, which was modelled by fixing the nodes adjacent to th pile in the alluvium and the Thames Gravel in the horizontal direction Excavation to the base of the Thames Gravels was then simulated b removing each element over one increment block. Where excavatio occurred under bentonite slurry, a load equivalent to the hydrostati pressure of the bentonite ($\gamma_b$ = 11 kN/m$^3$) was applied to the edge an base of the bore as each element was removed. In the analysis the tot. time for excavation to the base of the bore was 162 min and a furth time step of 20 min was allowed prior to placement of the concrete. Th. was typical of the actual construction time.

The wet concrete, which was taken to have a unit weight $\gamma_c$ c 24 kN/m$^3$, was placed from the bottom of the bore up, replacing th bentonite. As the concrete was poured, the displaced bentonite wa assumed to fill the temporary casing supporting the upper part of th bore so that the entire pile was poured under bentonite.

Concreting was modelled by increasing the pressures on the excavate faces as indicated in Fig. 17, following Lings *et al.* (1994). Wet-concret pressures equivalent to the hydrostatic pressure of the wet concrete plu the pressure due to the weight of the overlying bentonite slurry wer applied until a critical depth of concrete $h_{crit}$ was reached ($A_2B_2C_2$ i Fig. 17). The critical depth $h_{crit}$ was taken to be equal to one-third of th depth (6 m in this case), as suggested by Lings *et al.* (1994).

The wet-concrete pressures applied to the side of the bore durin concreting are summarized in Fig. 17. Prior to concreting, the initi pressures on the soil were those due to the static pressure of bentoni ($A_1B_1$). When the bentonite/concrete interface reached the critical dept of 6 m the lateral-pressure diagram was defined by $A_1B_2C_2$. As the dept of concrete was increased, the increase in lateral pressure with dept below $h_{crit}$ (measured from the current upper surface of the concrete) wa

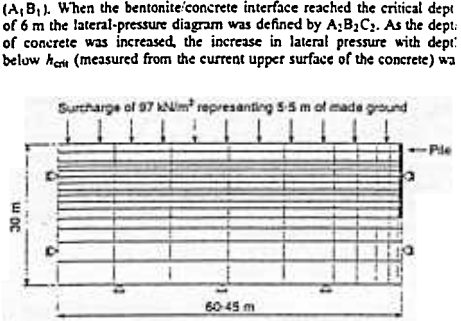


Fig. 15. Axisymmetric finite-element mesh

Table 5. Soil parameters used in axisymmetric finite-element analysis of installation effects for a single pile

| | $\varphi'$: ° | $E'$: MN/m² | $k$: m/s | $K_0$ |
|---|---|---|---|---|
| Made ground | 25 | 10 | $8 \times 10^{-4}$ | 0·5 |
| Alluvium | 25 | 1·8 | $1 \times 10^{-6}$ | 0·8 |
| Thames Gravels | 35 | 50 | $5 \times 10^{-4}$ | 0·5 |
| Lambeth Group Clays | 27 | 70 | $1{\cdot}2 \times 10^{-6}$ (h)† $1 \times 10^{-11}$ (v)† | 1·5 |
| Lambeth Group Sands | 30 | 250 | $2{\cdot}8 \times 10^{-6}$ (h)† $1 \times 10^{-7}$ (v)† | 1·5 |
| Thanet Sands | 33 | 300–450* | $2{\cdot}1 \times 10^{-5}$ | 1 |

* The stiffness increases from a minimum at the top of the stratum to a maximum at the base of the stratum.
† (h) and (v) indicate properties in the horizontal and vertical directions, respectively.

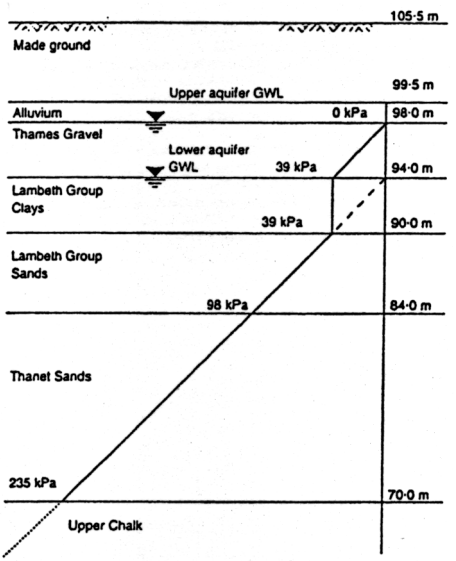


Fig. 16. *In situ* groundwater pressures assumed in analysis (GWL, groundwater level)

restricted to the unit weight of bentonite $\gamma_{bentonite}$ (e.g. $A_2B_3C_3C_2$ in Fig. 17). As the concrete pressures were applied over the upper part of the bore, the horizontal fixities of the adjacent nodes were released, simulating the removal of the casing. After the completion of concreting and withdrawal of the temporary casing, the final (maximum) lateral pressure diagram for the wet concrete was given by the line $A_2B_4C_2$.

Setting of the concrete was modelled over 28 days, during which time the wet-concrete pressures were gradually removed and elements representing the hardened concrete added.

### *Dewatering of lower aquifer level*

After a further 42 days the line of zero pore water pressure in the lower aquifer was lowered to 82 m TD to simulate the lowering of the groundwater level in the Thanet Sands and the Upper Chalk. This was modelled over a period of 50 days, which reflects the actual time taken to lower the water level on site. Pore water pressures at elevations between 82 m TD and the base of the Lambeth Group Clays at 90 m TD were set to zero. The pore water pressures and lateral stresses at the end of the wall installation analysis were then used as input data at the start of the main analysis.

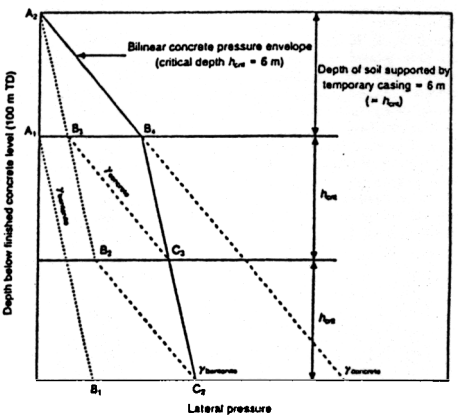


Fig. 17. Wet-concrete pressures on the side of the bore (after Lings *et al.*, 1994)

NOTATION

| | |
|---|---|
| $A$ | nominal cross-sectional area of prop |
| $E$ | Young's modulus |
| $E'$ | effective-stress Young's modulus |
| $f$ | gauge adjustment factor to eliminate temperature effects |
| $h_{crit}$ | critical depth of concrete (see Appendix) |
| $I$ | second moment of area |
| $K_0$ | *in situ* earth pressure coefficient |
| $K_a$ | active earth pressure coefficient |
| $K_i$ | pre-excavation earth pressure coefficient |
| $K_p$ | passive earth pressure coefficient |
| $k$ | permeability (subscript denotes direction: h, horizontal; v, vertical) |
| $P$ | average axial prop load |
| $P_M$ | measured prop load |
| $P_T$ | temperature-adjusted prop load |
| $T_D$ | datum temperature |
| $T_M$ | measured temperature |
| $\delta$ | soil/wall friction angle |
| $\gamma$ | unit weight |
| $\gamma_{bentonite}$ | unit weight of bentonite slurry |
| $\gamma_{concrete}$ | unit weight of concrete |
| $\nu'$ | Poisson's ratio |
| $\rho$ | bulk density of soil |
| $\epsilon_{av}$ | average measured strain |
| $\varphi'_{crit}$ | critical-state soil strength |
| $\varphi'_{mob}$ | mobilized soil strength |
| $\varphi'_{peak}$ | peak soil strength |

REFERENCES


Batten, M. (1998). *Prop loads in two large braced excavations*. PhD thesis, University of Southampton.

Batten, M., Powrie, W., Boorman, R. & Yu, H. T. (1996). Measurement of prop loads in a large braced excavation during the construction of the J.L.E. station at Canada Water, East London. In *Geotechnical aspects of underground construction in soft ground* (eds R. J. Mair and R. N. Taylor), pp. 57–62. Rotterdam: Balkema.

Batten, M., Powrie, W., Yu, H. T., Boorman, R. & Leiper, Q. (1999). Use of vibrating wire strain gauges to measure loads in tubular steel props supporting deep retaining walls. *Proc. Instn Civ. Engrs Geotech. Engng*, 137, Jan, 3–13.

Bolton, M. D. (1986). The strength and dilatancy of sands. *Géotechnique* 36, No. 1, 65–78.

Bolton, M. D. & Powrie, W. (1988). Behaviour of diaphragm walls in clay prior to collapse. *Géotechnique* 38, No. 2, 167–189.

Britto, A. M. & Gunn, M. J. (1987). *Critical state soil mechanics via finite elements*. Chichester: Ellis Horwood.

Burland, J. B. & Kalra, J. C. (1986). Queen Elizabeth II Conference Centre: geotechnical aspects. *Proc. Instn Civ. Engrs Part 1*, 80, December, 1479–1503.

Caquot, A. & Kerisel, J. (1948). *Tables for the calculation of passive pressure, active pressure and bearing capacity of foundations*. Paris: Gauthier-Villars.

Ferguson, P. A. S., Runacres, A. J. and Hill, N. A. (1991). London's Docklands: ground conditions and tunnelling methods. *Proc. Instn Civ. Engrs Part 1*, 90, December, 1179–1201.

Geotechnical Consulting Group (1991). *Jubilee Line Extension project, sectional interpretive report 2, Canada Water to Pioneer Wharf*. Geotechnical Consulting Group.

Gibson, R. E. (1953). Experimental determination of the true cohesion and true angle of internal friction in clays. *Proc. 3rd Int. Conf. Soil Mech. Found. Engng, Zurich*, 126–130.

Glass, P. R. & Powderham, A. J. (1994). Application of the observational method at the Limehouse Link. *Géotechnique* 44, No. 4, December, 665–679.

Gourvenec, S. M. (1998). *Three dimensional effects of diaphragm wall installation and staged construction sequences*. PhD thesis, University of Southampton.

Higgins, K. G., Potts, D. M. and Symons, I. F. (1989). *Comparison of predicted and measured performance of the retaining walls of the Bell Common Tunnel*, Contractor Report 12. Crowthorne: Transport and Road Research Laboratory.

Howland, A. F. (1991). London's Docklands: engineering geology. *Proc. Instn Civ. Engrs Part 1*, 90, December, 1153–1178.

Lings, M. L., Ng, C. W. W. and Nash, D. F. T. (1994). The lateral pressure of wet concrete in diaphragm wall panels cast under bentonite. *Proc. Instn Civ. Engrs Geotech. Engng* 107, No. 3, 163–172.

Marchand, S. P. (1997). Temporary support to basement excavations and strut load monitoring. *Proc. Instn Civ. Engrs Geotech. Engng* 125, No. 3, 1–14.

Ng, C. W. W., Lings, M. L., Simpson, B. & Nash, D. F. T. (1995). An approximate analysis of the three-dimensional effects of diaphragm wall installation. *Géotechnique* 45, No. 3, 497–507

Ove Arup and Partners (1991). *Jubilee Line Extension, sectional interpretive report 3, Isle of Dogs*. London: Ove Arup and Partners.

Page, J. R. T. (1995). *Changes in lateral stress during slurry trench wall installation*. PhD thesis, Queen Mary and Westfield College, University of London.

Powrie, W. (1996). Limit equilibrium analysis of embedded retaining walls. *Géotechnique* 46, No. 4, 709–723.

Powrie, W. & Li, E. S. F. (1991). Finite element analyses of an *in situ* wall propped at formation level. *Géotechnique* 41, No. 4, 499–514.

Powrie, W., Pantelidou, H. & Stallebrass, S. E. (1998). Soil stiffness in stress paths relevant to diaphragm walls in clay. *Géotechnique* 48, No. 4, 483–494.

Powrie, W., Chandler, R. J., Carder, D. R. & Watson, G. V. R. (1999). Back-analysis of an embedded retaining wall with a stabilizing base slab. *Proc. Instn Civ. Engrs Geotech. Engng*, 137, April, 75–86.

Twine, D. & Roscoe, H. (1997). *Prop loads: guidance on design*. CIRIA Core Programme Funders' Report FR/CP/48. London: Construction Industry Research and Information Association.